Results in Materials 17 (2023) 100358

Contents lists available at ScienceDirect

Results in Materials

journal homepage: www.sciencedirect.com/journal/results-in-materials

A novel carbon nanotubes doped natural rubber nanocomposite with balanced dynamic shear properties and energy dissipation for wave energy applications

Ali Esmaeili, Ian Masters, Mokarram Hossain *

Zienkiewicz Centre for Computational Engineering, Faculty of Science and Engineering, Swansea University, SA1 8EN, United Kingdom

ARTICLE INFO

Keywords:
Natural rubber
CNTs
Shear test
Payne effect
Mullins effect
Hysteresis loss
Energy dissipation

ABSTRACT

Mechanical characterizations of natural rubber filled with carbon-based nanomaterials were extensively studied in tensile and tear modes whereas fewer attempts have been conducted on a dynamic shear condition using a double-bonded shear test piece. This is of importance since natural rubbers are widely used as flexible membranes for wave energy harvesting devices. Therefore, this study was aimed to explore the microstructural, rheological, and dynamic viscoelastic characteristics of natural rubbers filled with different Multi-Walled Carbon Nanotubes (MWCNTs) contents. A combined compounding approach was employed to ensure a homogenous CNT dispersion was achieved. Transmission electron microscopy (TEM) was performed for the materials characterization while the processability and curing parameters of the compounds were investigated using the Mooney viscosity and rheometry test. Dynamic shear properties were compared using a cyclic test performed on a double-bonded shear test piece. TEM images showed that an optimum CNTs dispersion was reached at 3 phr MWCNTs loading whereas increasing CNT content resulted in further inhomogeneity. The addition of CNTs into the natural rubber not only improved the curing properties of the compound, i.e., low scorch and curing times, but it also increased the Mooney viscosity, the rheological properties, and the dynamic shear properties of the nanocomposite compared to the pristine rubber. The Payne and Mullins effects were also observed for all compounds manifesting dependency on the CNTs content and applied strain amplitude. Finally, MWCNT enhanced the dissipated energy of the nanocomposites with respect to the neat rubber in which an increase of 1040 % in energy dissipation for 10 phr MWCNTs compared to the control at a strain amplitude of 200 % was achieved.

1. Introduction

Rubber-like materials such as natural rubbers (NR) have been widely used in different industrial applications including flexible membranes for wave energy harvesting [1], vibration and shock absorbers [2], tires [3], and soundproofing systems [4,5]. Due to the broad range of applications, investigations have been conducted on filled and unfilled natural rubbers to understand their rheological and mechanical behaviour [6–9]. Further, the development of nanomaterials has led to polymer nanocomposites; novel materials with multifunctional properties. Carbon nanotubes (CNTs) are one of the most promising one-dimensional (1D) nanomaterials with outstanding capabilities in tailoring multifunctional properties of polymer-based materials due to their large aspect ratio and surface area, excellent electrical and thermal conductivities, and excellent mechanical properties [10]. Consequently, numerous efforts have been attempted to combine natural rubbers with CNTs to improve their performance including mechanical and rheological characteristics [11–15].

Very recently, several companies proposed the use of natural rubber-based flexible membranes for energy harvesting applications and a number of large scale prototypes have been demonstrated. However, fatigue life of natural rubber is still a major issue in energy harvesting applications [1]. Hence, the enhancement of their fatigue life by incorporating CNTs has been addressed in the literature which was attributed to crack branching and crack deviation [16–19]. Submerged in the harsh environment of the ocean, a flexible membrane experiences complex modes of deformation (e.g., tension, compression, shear); therefore, it is necessary to characterise CNTs-NR in a complex mode of

* Corresponding author.
E-mail address: mokarram.hossain@swansea.ac.uk (M. Hossain).

https://doi.org/10.1016/j.rinma.2022.100358
Received 28 October 2022; Received in revised form 7 December 2022; Accepted 12 December 2022
Available online 14 December 2022

deformations. Further investigation is needed to establish the relationship between CNT content and the dynamic mechanical properties of the filled rubbers at various levels of strains and strain rates. In particular, Payne and Mullins effects under double bonded shear test require further investigation. As the first step, viscoelastic characterization of CNTs-filled rubber will be identified using a double-bonded shear test under cyclic loading-unloading conditions.

Sethulekshmi et al. [20] have recently conducted an extensive review focusing on the reinforcing capability of various nanofillers, e.g., CNTs, Graphene Nanoplatelets (GNPs), nanoclay, and titanium oxides (TiO_2) for natural rubber-based nanocomposites. According to their results, CNTs have shown great potential in enhancing the mechanical and electrical performance of natural rubbers at relatively low content compared to other conventional fillers such as Carbon Black (CB), which require much larger content. Mensah et al. [21] studied important parameters in reaching appropriate mechanical properties of CNT-reinforced elastomers in terms of their morphologies, functionalizations, dispersion of CNTs, and their compounding techniques, i.e., solution mixing or mechanical/melt mixing techniques. It was concluded that the effective addition of CNTs resulted in enhanced mechanical properties. Nevertheless, it was strictly dependent on the compounding techniques used. It is worth noting that although the melt mixing method is the most widely used technique in the rubber industry, its efficiency for the CNT dispersion is still disputable. Therefore, some studies used a combination of both melting and solution mixings to reach better CNTs dispersion [14,22].

Although several studies have been conducted on the mechanical characterization of natural rubbers filled with nanomaterials in tensile and tear modes [23–27], very few attempts have been conducted on double bonded shear condition which is a typical loading condition for bearing and anti-earthquake applications [28–30]. Anisotropic properties of natural rubbers filled with CNTs through in-plane and in-thickness directions were studied using double bonded shear test indicating an orthotropic and transversally isotropic material behaviour [28]. They found that decreasing CNTs content led to a more anisotropic response, especially in Payne effect resulting from rearrangement of CNTs when subjected to low and medium strain levels. They have also conducted a further study in which the dynamic shear properties of silica-based hybrid fillers based natural rubber nanocomposites under double bonded shear conditions were investigated [29]. Ismaili et al. [30] have investigated shear modulus and damping ratio of CNT-filled natural rubber using a double bonded shear test. Despite the fact that the aforementioned studies conducted dynamic double bonded shear condition tests, no rigorous discussions were made on the Payne and Mullins effects, hysteresis loss and energy dissipation with respect to CNT contents and synthesis methods used. In addition, the scope of those works was limited to intermediate strain levels whereas the real service condition for many engineering applications such as in flexible wave energy converters (WECs) is much higher.

Therefore, the current study aims to investigate the effects of MWCNTs on the microstructural, rheological, and dynamic mechanical properties of natural rubbers. F Different CNT contents, i.e., 1 phr, 3 phr, 5 phr, and 10 phr along with the control (EDS35) were studied so that an optimum CNTs content can be obtained resulting in appropriately balanced microstructural, rheological and mechanical properties. Due to the high tendency of CNTs to aggregate, a combined rubber compounding approach, i.e., solution and melt mixing methods were used for the rubber compounding to ensure a homogenous CNT dispersion can be achieved. Transmission electron microscopy (TEM), Mooney viscosity, and rheometry analyses were performed for the materials characterization while a cyclic double-bonded shear test was conducted for the mechanical characterization. Consequently, dynamic shear properties including complex modulus, storage and loss moduli, loss angle, and energy dissipation of various natural rubber compounds were compared as a function of CNTs content and applied shear strains.

2. Natural rubber/CNTs preparation

2.1. Materials and Master Batch preparations

Natural rubber *SMR CV60* was provided from a Malaysian rubber company (denoted as NR) and *NC7*000TM MWCNT purchased from *Nanocyl* with an average diameter and length of 10 nm and 1.5 μm, respectively, was used for these experiments. A Master Batch (MB) containing 10 phr CNT was prepared as follows. First, NR was cut into small pieces (Fig. 1 a) and then dissolved into toluene with the weight ratio of 325:3250 g (NR toluene) and left for four days to turn into a viscous mixture (Fig. 1b). It is worth noting that some NRs coagulated and deposited on the bottom of the tin over time as shown by the green arrow in Fig. 1c. Hence, the NR/toluene solution was further stirred for 1 h using a compressed air drill mixer before adding CNT into the mixture. In addition, CNT (32.5 g) were mixed into 750 ml toluene and then bath sonicated for 30 min followed by the addition of the CNTs/toluene mixture to the NR/toluene solution and stirred for another hour using an air drill mixer for a better homogenization (Fig. 1d). The mixture was dried at room temperature in a tray for two days and subsequently peeled off as shown in Fig. 1e-g, respectively. The samples were further homogenized and degassed using a two-roll mill (Fig. 1 h-i) resulting from extreme shear forces applied by the mill.

2.2. NR/CNTs compounding

The MB was further diluted during the rubber compounding using the pristine CV60 to achieve the desired CNTs content, i.e., 1 phr, 3 phr, and 5 phr. Therefore, five different batches including control (batch1), 1 phr (batch2), 3 phr (batch3), 5 phr (batch4), and 10 phr (batch5) were prepared. Table 1 shows the formulation of the rubbers in which the MB was diluted by NR (CV60) depending on the desired CNT' content. It is worth noting the MB contains 10 wt% CNTs. The rubber compounding was carried out using an internal mixer *Polylab OS* and a two-roll mill (*David Bridge*). First NR/MB was added to the internal mixer and mixed for 2 min followed by adding zinc oxide, stearic acid, 6PPD, and Sasol Wax for another 5–6 min mix; then the compounded rubber was dumped. It is worth noting that the torque and temperature of the compound throughout the mixing by the internal mixer were monitored to avoid overheating. Subsequently, Sulfur and CBS were added to the dumped compound on the mill resulting in crosslinking and further homogenization. The mill was carried out several times until the sample reached proper homogenization. The samples were weighed before and after each process to monitor further drying of the compound. It should be noted that no MB was used for batch 1 whereas 110 ph MB was employed for batch 5.

2.3. Mooney viscosity, rheometry test, and final curing

Processing properties of the compounds was identified by conducting the Mooney viscosity at 100 °C and constant speed of 2 rpm for 5 min, 1 min preheating and 4 min test, using a sample of 25 g. The rheometry analysis was also carried out to obtain the vulcanization parameters in which a sample of 5 g is rotated 6° clockwise and anticlockwise for 30 min throughout the rheometry test. The vulcanization parameters were obtained using rheometry tests. For that, a square sample with the dimension of 9″ x 9" x 2 mm was produced using a mould.

2.4. Characterization

A double-bonded shear test piece was prepared using the mould shown in Fig. 2a in which the diameter and thickness of the disk after molding is 25 mm and 6 mm, respectively (Fig. 2b). The doubled-bonded shear test pieces were cured at 150 °C for 30 min. A sinusoidal waveform at 1 Hz with a temperature of 24 °C was applied to the specimen using a *Dartec* servohydraulic testing machine at the strain amplitudes (%) of 1,

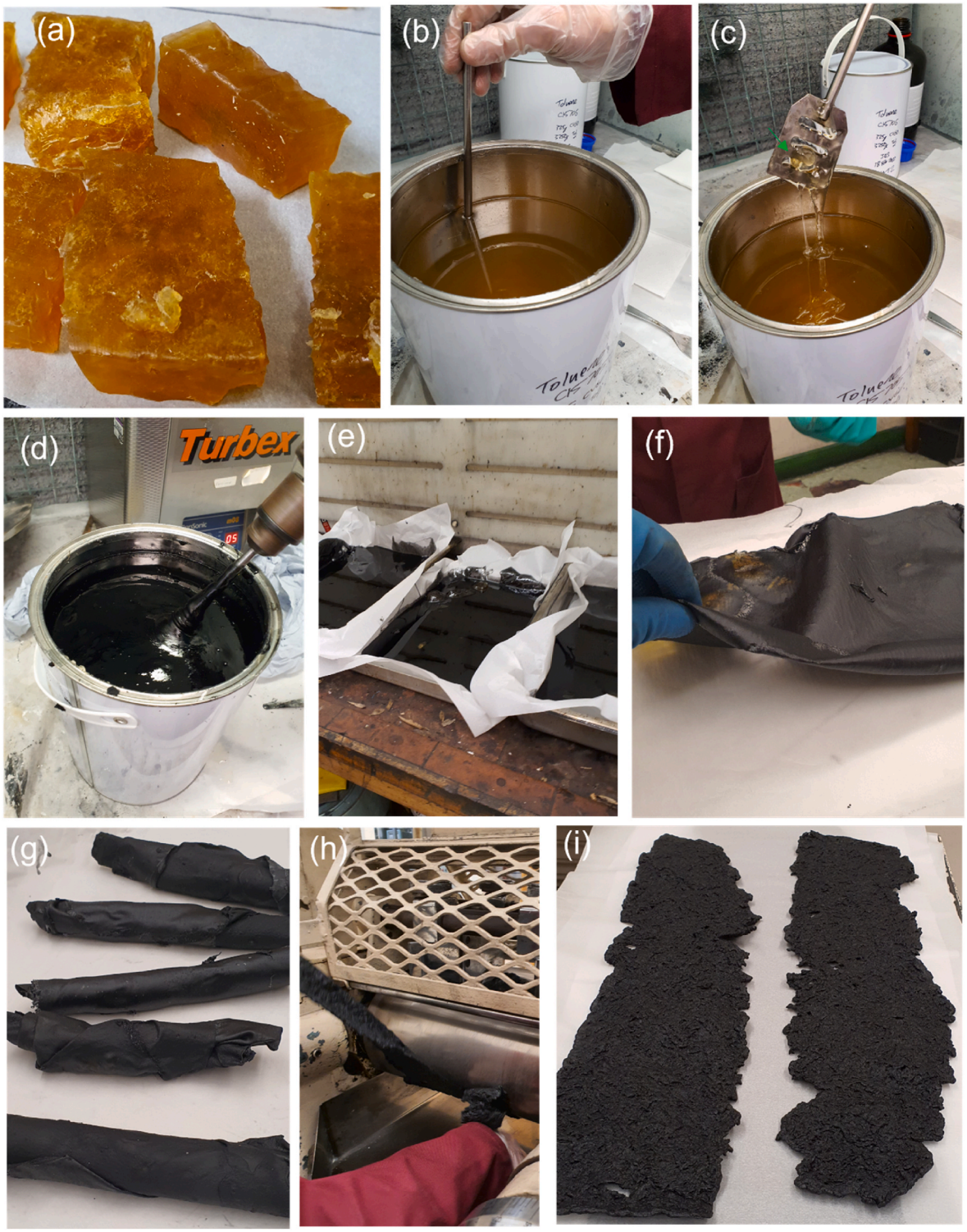

Fig. 1. MB preparation: (a) cutting SMR CV60 into small pieces, (b) formation of a viscous based liquid CNT/NR solution by dissolving CV60 into toluene, (c) presence of lumps resulting from coagulation of some CV60, (d) CNTs addition into the NR/toluene solution, (e) drying of CNT-CV60/toluene in a tray, (f–g) peeling off the CNT/NR film from the baking paper, (h) further homogenization of NR/CNT MB using two-roll mill (j) MB.

2, 5, 10, 50, 100, 150, and 200 for 6 consecutive cycles (Fig. 2c–e) at each strain amplitude and 1 min rest between each step. This procedure was performed to investigate the effect of strain history on the dynamic properties of the materials. The test was repeated to ensure the results are repetitive; therefore, the dynamic shear properties are reported for both first and second runs. In other words, the test, in total, was composed of 37 steps with 1 min rest time between each step and 108 cycles as shown in Fig. 2d. The absolute value of complex dynamic shear modulus (MPa) hereinafter called the complex modulus, dynamic shear storage modulus (MPa) hereinafter called the storage modulus, and the dynamic shear loss modulus (MPa) hereinafter called the loss modulus were obtained from equations (1)–(3), respectively:

Table 1
Rubber formulation (phr).

Batch No	NR	MB	Zinc oxide	Stearic acid	6PPD	Sasol wax	CBS	Sulfur	Density (g/cm^3)
1	100 (290)	0 (0)	5 (14.5)	2 (5.8)	3 (8.7)	2 (5.8)	1.5 (4.35)	1.5 (4.35)	0.968
2	89 (258.1)	12 (34.8)	5 (14.5)	2 (5.8)	3 (8.7)	2 (5.8)	1.5 (4.35)	1.5 (4.35)	0.972
3	67 (194.3)	36 (104.4)	5 (14.5)	2 (5.8)	3 (8.7)	2 (5.8)	1.5 (4.35)	1.5 (4.35)	0.978
4	45 (130.5)	60 (174)	5 (14.5)	2 (5.8)	3 (8.7)	2 (5.8)	1.5 (4.35)	1.5 (4.35)	0.985
5	0 (0)	110 (319)	5 (14.5)	2 (5.8)	3 (8.7)	2 (5.8)	1.5 (4.35)	1.5 (4.35)	1.001

The unit in the parenthesis is gram

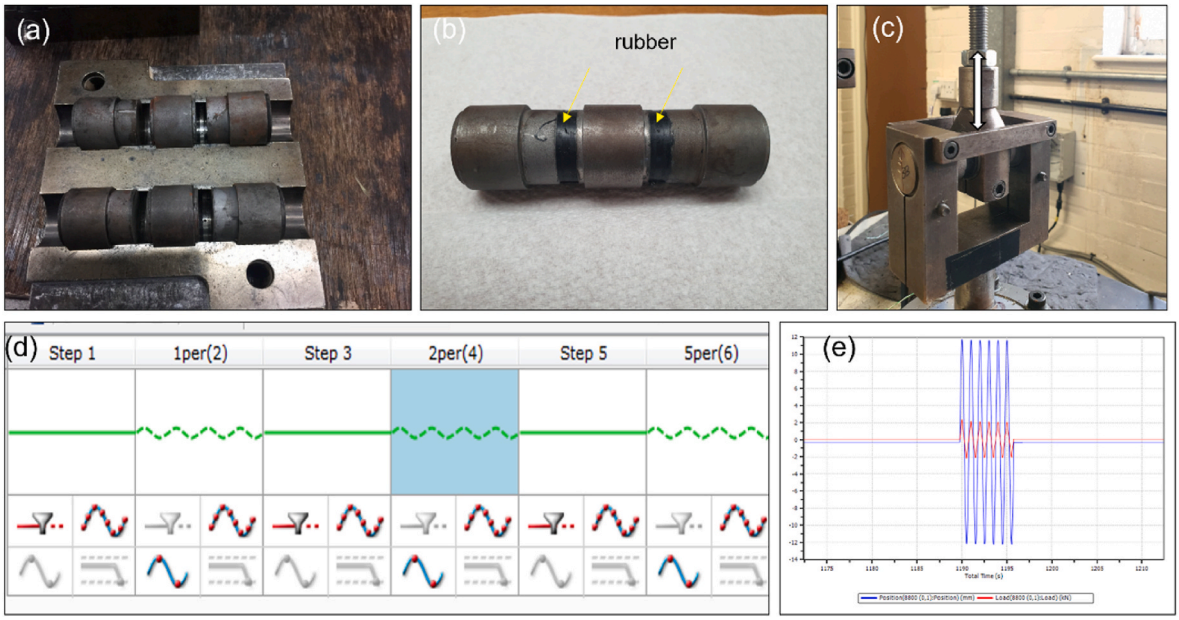

Fig. 2. Doubled bonded shear test preparation: (a) the mould, (b) the test piece after molding, (c) test setup, (d) steps of the test, (e) 6 cycles for each strain amplitude.

$$G^* = \frac{Kh}{2A} \tag{1}$$

$$G' = |G^*| cos\ \delta \tag{2}$$

$$G'' = |G^*| sin\ \delta \tag{3}$$

where K is the stiffness (KN/mm), h is the thickness (mm), δ is the loss angle, and A is the cross-section (mm^2). Finally, the energy dissipation (mJ/cycles), quantified by the area of the hysteresis loop, was obtained to compare the energy dissipation as a function of CNTs' content.

3. Results and discussions

3.1. Microstructural characterisation

Fig. 3 shows the dispersion state of CNTs within the NR at different CNT loadings in which left and right column figures represent low and high TEM magnifications, respectively. The presence of poor-CNTs regions highlighted by yellow arrows in Fig. 3a and b can be distinguished whereas no CNTs bundles can be observed for 1 phr CNT loading resulting from a relatively low amount of the nanofillers used for batch 2. On the other hand, 3 phr CNT loading manifests excellent nanofillers dispersion, i.e., neither poor-CNTs regions nor CNTs aggregates can be detected (Fig. 3 c-d). Further addition of the CNTs up to 5 phr loading causes more heterogeneity in the samples leading to the presence of both CNTs aggregates and poor-CNTs regions as shown by red and yellow arrows in Fig. 3e and f, respectively. Similarly, CNTs agglomeration can be found for 10 phr CNTs as shown by red arrow in Fig. 3g and h, though it shows relatively a better CNTs dispersion with respect to 5 phr CNT loading.

3.2. Internal mixing monitoring

As it is mentioned earlier that the incorporation of NR and MB was conducted during the first 2 min of the mixing in the *Polylab OS* internal mixer followed by the addition of other ingredients. Hence, the internal mixing parameters including torque, temperature, and subsequently the energy consumption during the first 2 min of the mixing are shown in Fig. 4 to compare only the effects of CNTs incorporation on the mixing parameters before adding any other ingredients. Regardless of the type of the compound, the torque rises dramatically to the peak value at the beginning of the mixing resulting from high friction and shear forces required to breakdown the long polymer chain followed by a steady-state decrease forming a plateau which can be attributed to further homogenization of the compound throughout the mixing [31]. It is worth noting that the decrement rate of the torque following the peak value for the control and low CNTs contents (1 phr and 3 phr) are slightly quicker than the high CNTs loading (e.g., 5 phr and 10 phr) which can be related to the larger reinforcing effect when a higher CNTs content is used. Unlike the torque-time curves which shows a plateau, the temperature-time curves manifest an increasing trend throughout the mixing (Fig. 4a) arising from high shear forces during the mixing [15]. The energy consumption during the mixing is depicted in Fig. 4b indicating a higher energy consumption by the addition of CNTs; nevertheless the difference between the control, 1 phr, 3 phr, and 5 phr are not notable. It can be concluded that the incorporation of CNTs into the NR causes an increase in the required torque and energy

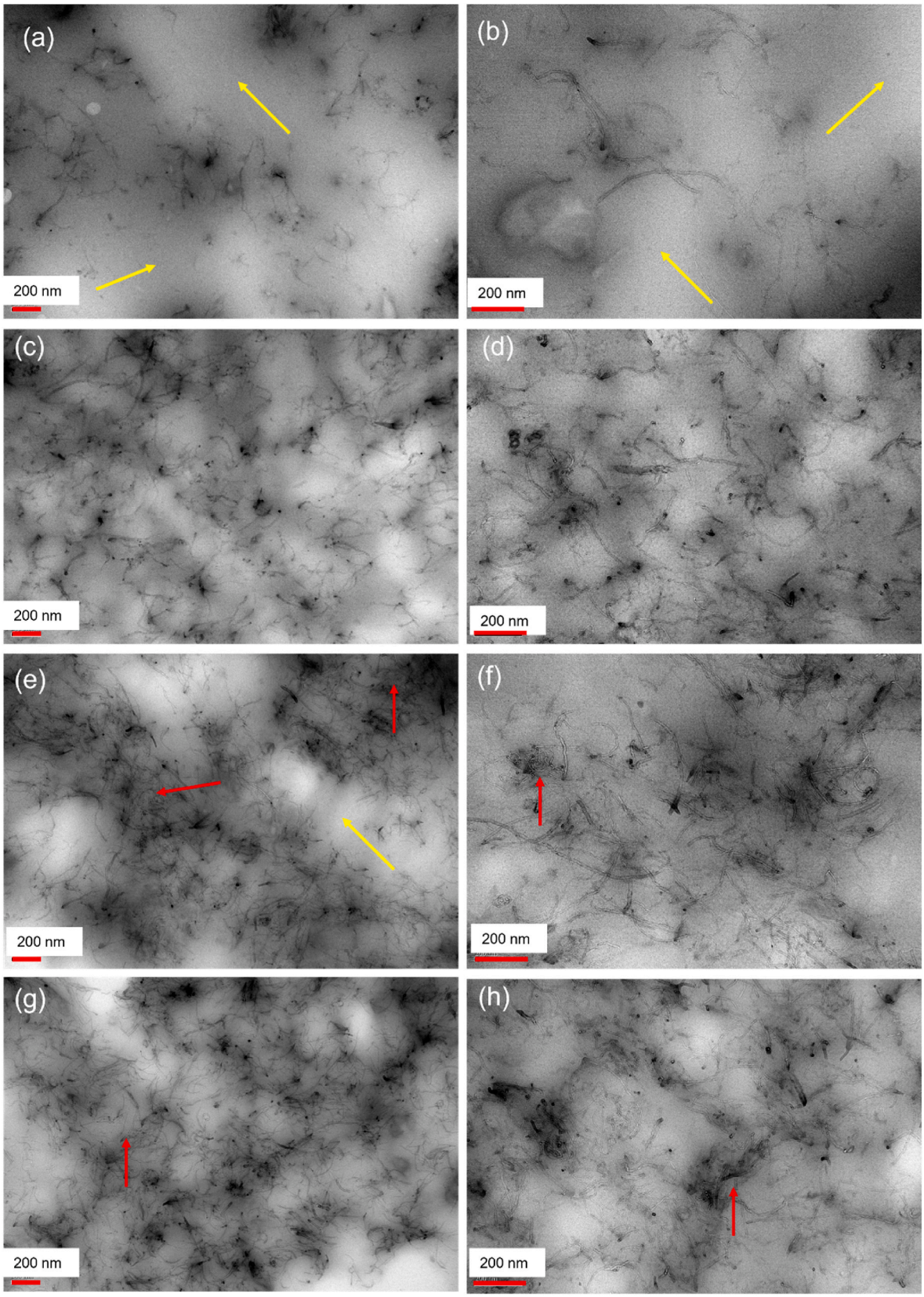

Fig. 3. TEM images of CNTs dispersion within the NR: (a–b) 1 phr, (c–d) 3 phr, (e–f) 5 phr, (g–h) 10 phr. The left and right columns figures are low and high magnification images respectively. The scale for all figures is 200 nm. The magnification for the left and right columns figures are 60,000 and 100,000 respectively.

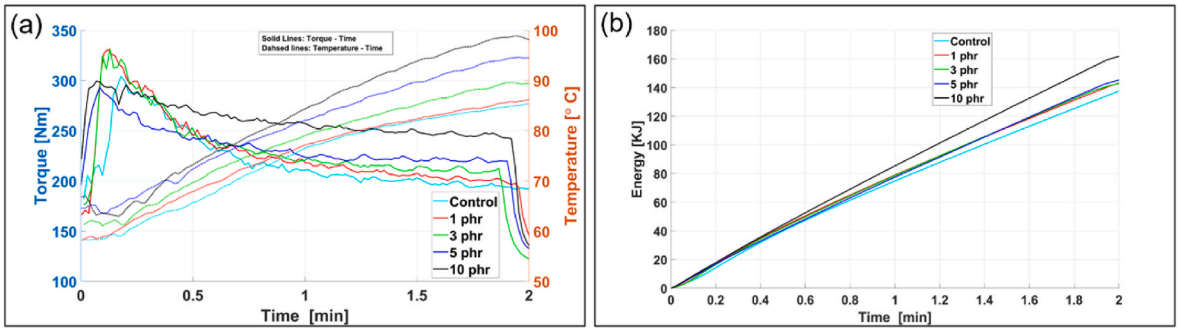

Fig. 4. Internal mixing parameters during the first 2 min: (a) the torque-time and the temperature-time curves, (b) the energy consumption versus time.

consumption during the mixing, in particular at a higher CNTs loading.

3.3. Mooney viscosity

The relationship of the macromolecular structure of the CNTs-filled natural rubbers with viscosity is usually studied via the Mooney viscosity test. The Mooney viscosities of the compounded rubbers along with the MB and the NR (the initial gum) are listed in Table 3. The NR and control possess the highest and the lowest Mooney viscosities, respectively, while the addition of 10 wt% of CNTs into the NR significantly reduces the Mooney viscosity resulting from the homogenization made by the two-roll mill. In addition, the incorporation of CNTs into the control (batch 1) increases the Mooney viscosity up to 200% at 10 phr CNTs loading (batch 5)with respect to the control due to hydrodynamic effect, i.e., the filler impedes the flow of rubber [32]. On the other hand, a significant reduction in the Mooney viscosity of the cured rubbers (batch 1 to 5) compared to the MB and CV60 can be distinguished which can be attributed to the further processing of the former with respect to the latter by the internal mixer and the twin-roll mill, i.e., the more the processing the lesser the viscosity.

3.4. Curing properties

Fig. 5a shows the vulcanization curves, i.e., torque-time relationships of the neat and filled rubbers. The torque-time curves can be distinguished into three different regions including induction or scorch region, curing region, and the post-curing region. It can be concluded that the scorch time (ts2) decreases with the CNTs addition, i.e., premature vulcanization takes place faster for CNTs-filled rubber compared to the control. Similarly, the time for 95% curing (i.e., t95) diminishes as a function of CNTs increasing (Fig. 5a and b). This can be attributed to enhancing the thermal conductivity of the CNTs-filled rubber, thus expediting the start of curing [15,33]. The minimum and maximum torques, ML and MH, respectively, increase for the filled rubbers with respect to the neat rubber (Fig. 5a and c). This indicates that the incorporation of CNTs enhances the stiffness during crosslinking, thus, more resilience can be seen. Addition of CNTs not only increases the MH values but also grows the minimum torque required (ML) resulting in better processability and viscosity. It is worth noting that the ML value represents the processability and viscosity of the compound [34]. The ML values obtained from rheometry are in good agreement with the viscosity of the compound obtained from the Mooney viscosity test in which the viscosity of the compound increases with the CNTs addition. The crosslink density, the difference between ML and MH, also increases with the CNTs addition in which batch 5 manifests the highest crosslink density (Fig. 5c). This indicates that CNT-filled natural rubber not only manifests smaller scorch and curing times, i.e., less energy is needed throughout the processing, but they can also increase the shear modulus due to a higher crosslink [34].

Table 3
The Mooney viscosities of unfilled and filled rubber including MB and NR.

Batch No.	1	2	3	4	5	MB	NR
Mooney viscosity (ML)	13	20.5	23	26.5	39	92	100.3

3.5. Mechanical properties

In order to understand the effects of CNTs on the NR, a series of mechanical experiments were conducted using a double-bonded shear test set-up. Fig. 6 shows the dynamic shear properties of the unfilled and filled rubbers at different strain levels for the first and second repeats of the test. Regardless of the strain level, the incorporation of CNTs into natural rubber increases the dynamic shear properties. In comparison with the control, the storage modulus, the loss modulus, the complex modulus, and the loss angle of filled-rubbers are increased up to 201%, 1232%, 202%, and 339%, respectively, for 10 phr CNTs loading at 200% strain amplitude (first run). The shear properties slightly decrease in the second run compared to the first run, i.e., an increase of 178%, 1092%, 328%, and 178% are achieved for the storage modulus, the loss modulus, the complex modulus, and the loss angle, respectively, which are slightly lower than the ones obtained in the first run. On the other hand, no significant change in the shear properties of the control can be seen for the first and second runs which can be related to the presence of no CNTs, so that, the stress-softening and Mullins effects can be neglected. It can be concluded that the addition of CNTs not only increases the storage modulus of the control, but it also increases the damping capability of the compound, i.e. the loss modulus increases which is an important property of the elastomers for energy absorption applications. The dynamic shear properties achieved in this study are in line with the rheometry outcomes, i.e., the higher the MH, the higher the modulus. The remarkable enhancement of the storage modulus by CNTs addition indicates a proper interfacial bonding between CNTs (filler) and natural rubber (matrix), leading to appropriate interfacial shear loading transfer [13].

Fig. 7 shows the changes in the storage and the loss moduli with the strain increase for unfilled and CNTs-filled rubbers [35]. The storage modulus decreases with increasing strain amplitude whereas the loss modulus manifests an increase followed by a decrease. Specifically, the storage modulus reduces dramatically at some critical strain levels (approximately at 10%) whereas the loss modulus manifests a peak as shown in Fig. 7. This can be attributed to the strain-softening effect known as the Payne effect indicating dependency of the storage and the loss moduli to the applied strain amplitude [36]. Destruction of the CNTs networks in the preliminary stage of deformation and their reconstructions at strain of 10% account for the peak in the loss modulus [37]. Note that the Payne effect can be quantified using the following equation (4) [37]:

$$\Delta G' = \frac{G'_{0.1\%} - G'_{10\%}}{G'_{0.1\%}} \quad (4)$$

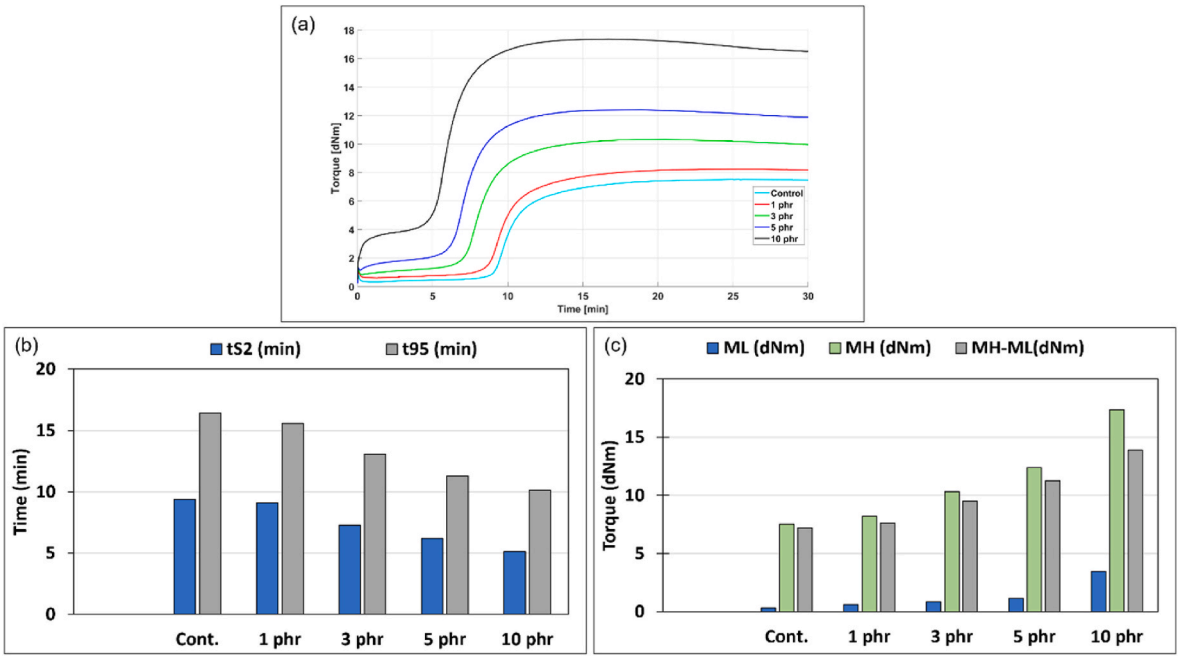

Fig. 5. Rheometry results: vulcanization curve of the unfilled and filled rubbers, (b) inducting and curing times (c) MH, ML, and MH-ML.

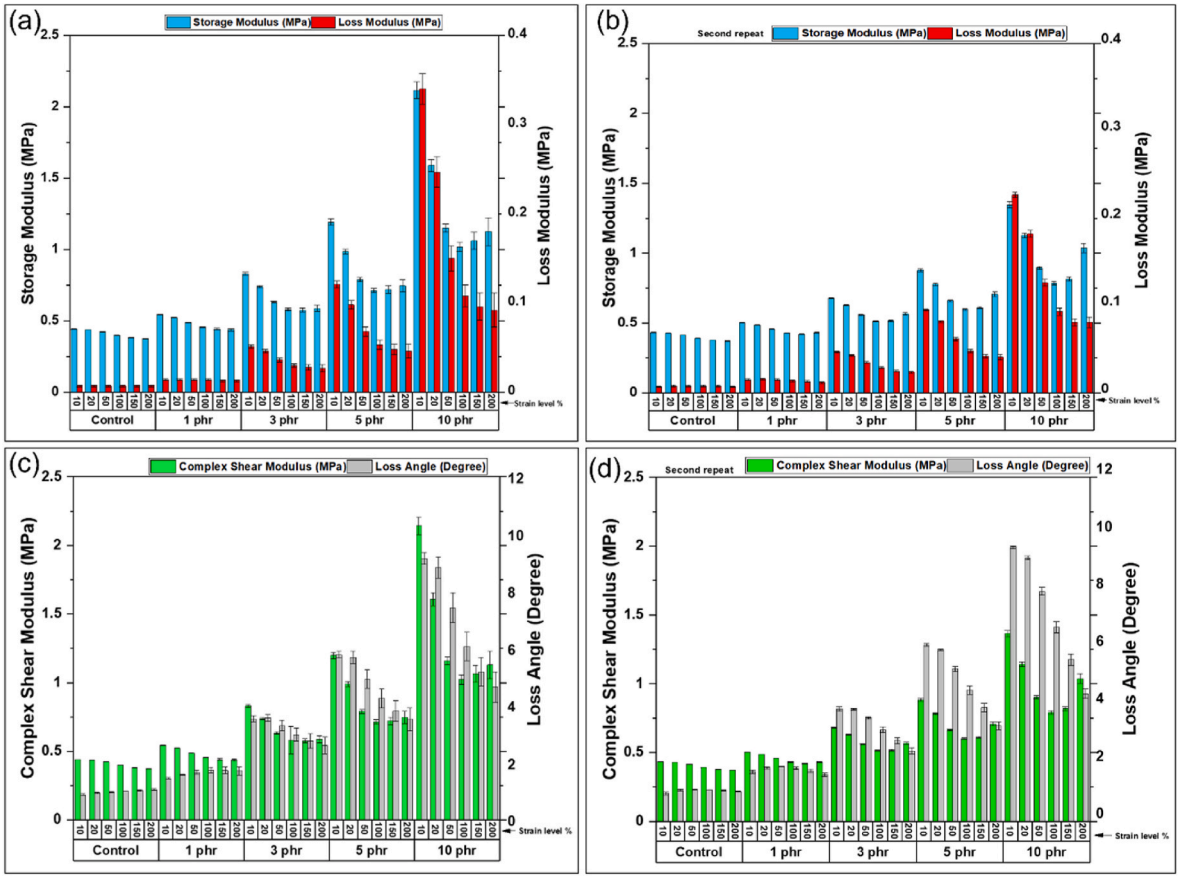

Fig. 6. Dynamic Shear properties of unfilled and filled natural rubber with CNTs at different strain levels: (a–b) the storage modulus and the loss modulus, (c–d) the complex modulus and the loss angle. The left and right column figures refer to the first and second test runs respectively.

where $G'_{0.1\%}$ is the storage modulus at 0.1% strain, $G'_{10\%}$ is the storage modulus at 10% strain, and $\Delta G'$ is the normalized Payne effect.

The Payne effects for batch 1 to 5 are 0.06, 0.05, 0.2, 0.35, and 0.5, respectively. No significant difference between the control and 1 phr CNT loading can be seen which can be attributed to low amount of CNTs used. 3 phr CNTs content manifests a relatively higher Payne effect with

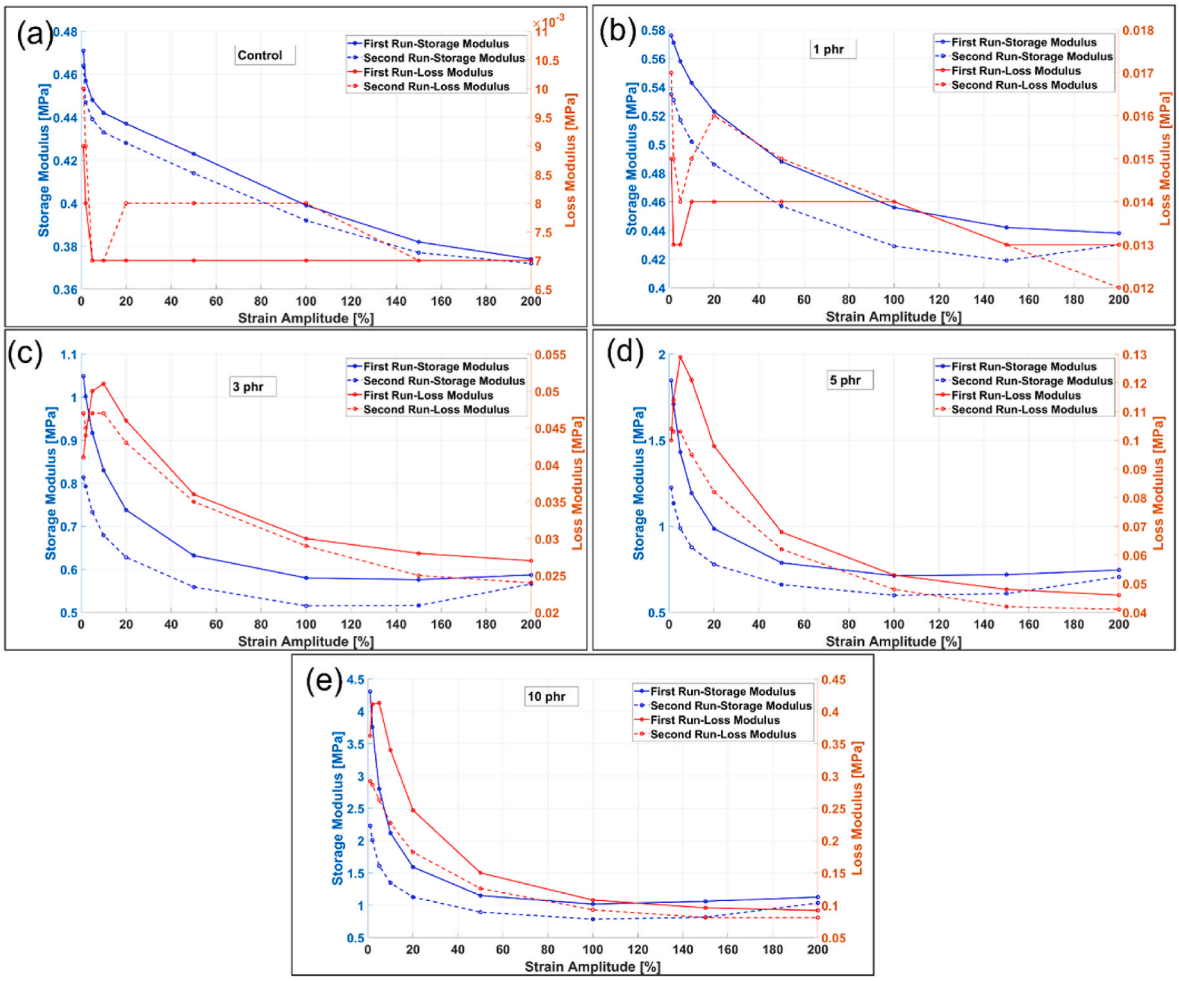

Fig. 7. The dynamic and the loss moduli as a function of strain amplitude manifesting the Payne effect: (a) control, (b) 1 phr CNTs, (c) 3 phr CNTs, (d) 5 phr CNTs, (e) 10 phr CNTs.

respect to 1 phr CNTs (300% increase). The Payne effect is more significant for higher CNT loadings (5 phr, and 10 phr) as shown in Fig. 7d and e i.e. the higher the CNT contents the higher the Payne effect because the agglomerated CNTs disentangle sufficiently during the initial stretching (strain <10%) resulting in further reductions of the shear modulus with respect to the strain increase [17]. This is in line with the literature indicating a higher Payne effect can be identified by increasing the filler loadings [38]. .

As it was mentioned before, the Payne effect is the strain-dependent properties of filled rubbers subjected to a relatively low amount of strain whereas the Mullins effect, also known as the stress-softening effect, can be distinguished at intermediate strain value [38]. Fig. 8 depicts the force-displacement for five successive cycles at strain of 50% (cycles 31 to 35) to compare the Mullins effect. Apart from the control and 1 phr CNTs in which no significant cyclic stress-softening can be found; other batches (3 phr, 5 phr and 10 phr) manifest obvious Mullins effects. That is, a large stress drop from the first to second loading cycles can be distinguished in the loading curves followed by a negligible reduction in the subsequent cycles resulting in steady state hysteresis loop in the 5th cycle.

Note that the presence of a stabilized loading-unloading curve from 5th onward is well-addressed in the literature resulting in the removal of the Mullins effect after specific cycles in the filled rubbers [39]. In addition, increasing the CNT content results in a more pronounced Mullins effect, in particular for 5 and 10 phr CNTs contents as shown in Fig. 8d and e which can be ascribed to detachment of CNTs or their slippages from the matrix [40,41]. Since hysteresis increases with increasing CNTs content, one can say that the Mullins effect is strongly related to filler-polymer chain interactions.

Since the hysteresis loss depends on the CNTs content as well as the applied strain, they are compared individually in response of the CNTs content (Fig. 9) and the applied strain (Fig. 10). Fig. 9 depicts the force-displacement relationships in a single loading-unloading cycle at different strain amplitudes including 50%, 100%, 150%, and 200%, respectively, to compare the dissipation behaviour as a function of the CNTs content. It should be noted that the same number of loading cycles was selected at each strain amplitude to avoid the effect of strain history on the hysteresis behaviour. The presence of the hysteresis loop can be clearly seen for both filled rubbers which is related to first feature of the Mullins effect, i.e. a considerable stress-softening during unloading with respect to the loading, in particular when the elastomer is subjected to a high strain deformation [41,42]. In fact, with the addition of CNTs, two distinct features can be distinguished in the loading-unloading curves including a larger hysteresis loss and a pronounced nonlinearity at high strain amplitude as shown in Fig. 9.

The hysteresis shown in Fig. 9 indicates irreversible dissipated energy resulting in heat generations in the materials which can be detrimental for the fatigue properties of the rubber [19]. It can be concluded that although incorporation of the CNTs into NR increases the dynamic shear properties as shown in Fig. 6, it also reduces the strain energy released during the unloading, i.e., the hysteresis and energy dissipation of the material increases by CNTs addition.

Fig. 10a–d shows the change in the hysteresis loop in response of the applied strain for each sample indicating a larger hysteresis loss by

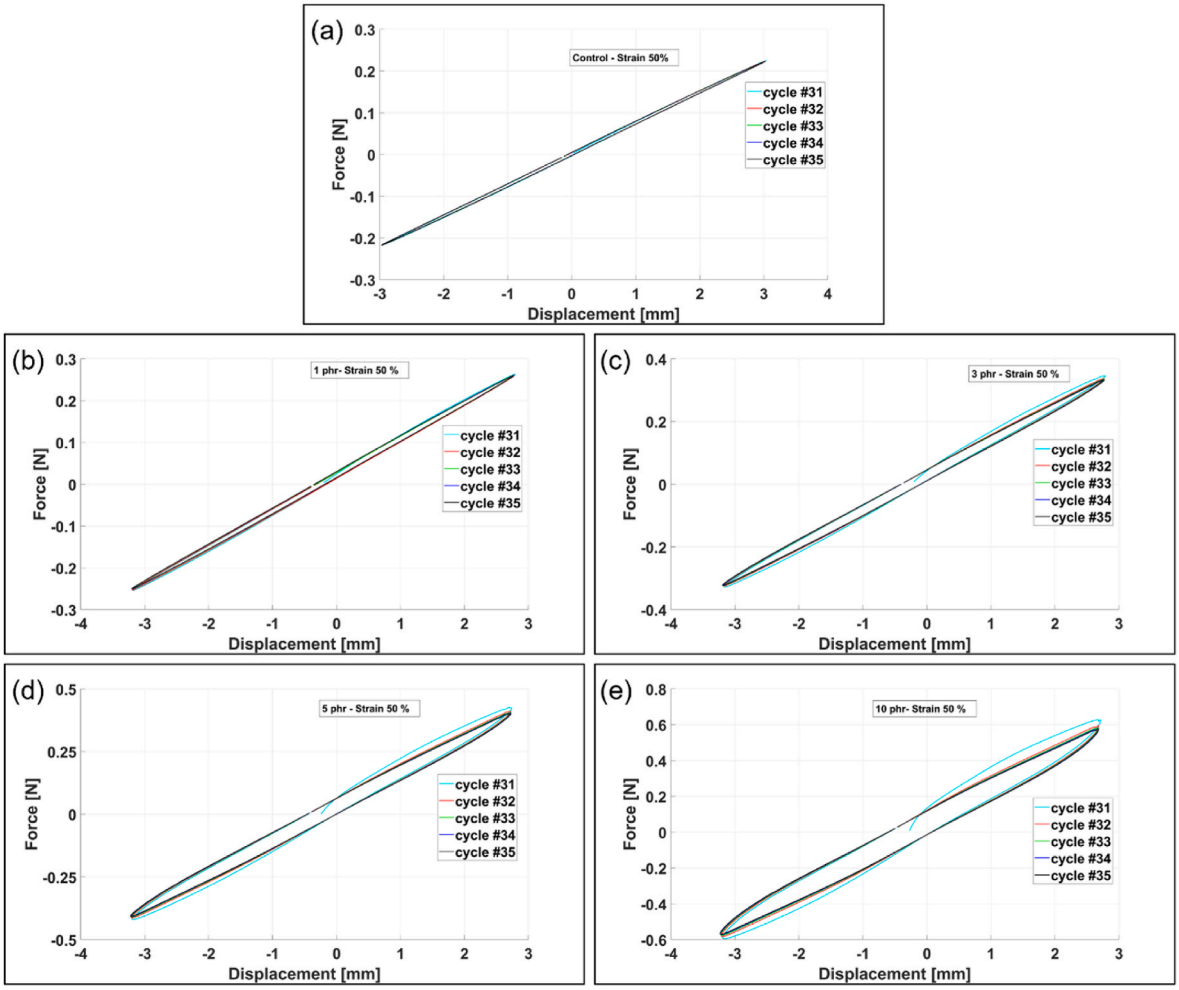

Fig. 8. Five consecutive shear loading-unloading representing the Mullins effect: (a) control, (b) 1 phr, (c) 3 phr, (d) 5 phr, (e) 10 phr.

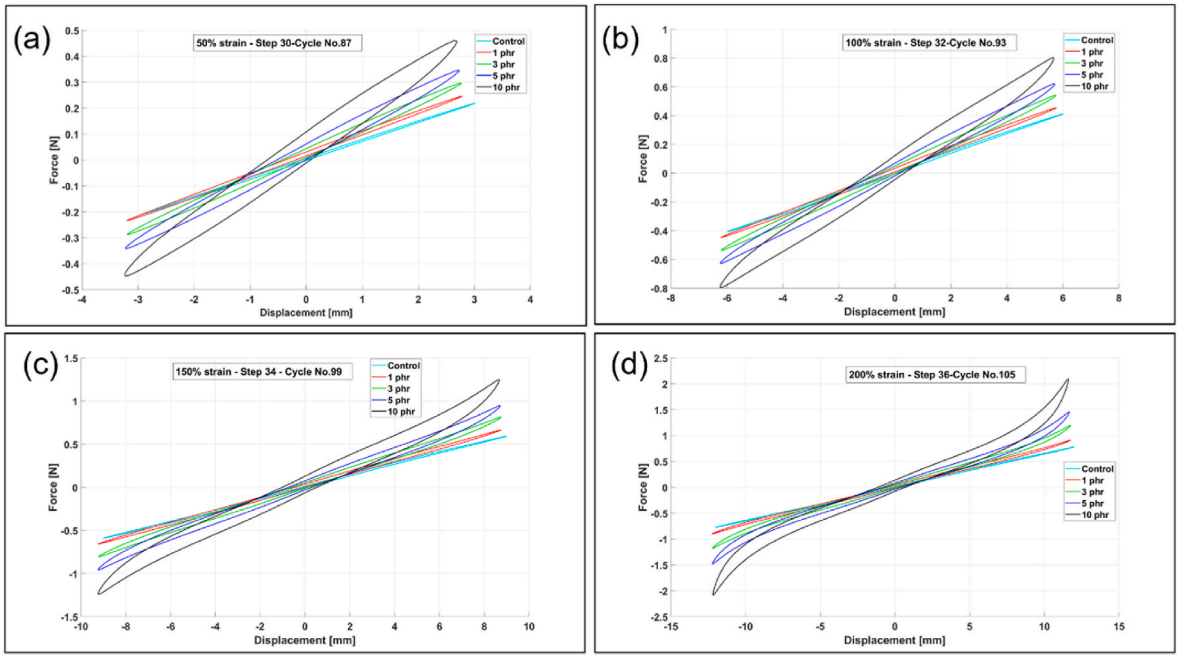

Fig. 9. Comparison of hysteresis loop for a single loading cycle as a function of CNTs content at different strain amplitude: (a) 50%, (b) 100%, (c) 150%, (d) 200%. The test is comprised of steps which are either rest periods or 6 loading cycles as shown in Fig. 5(d).

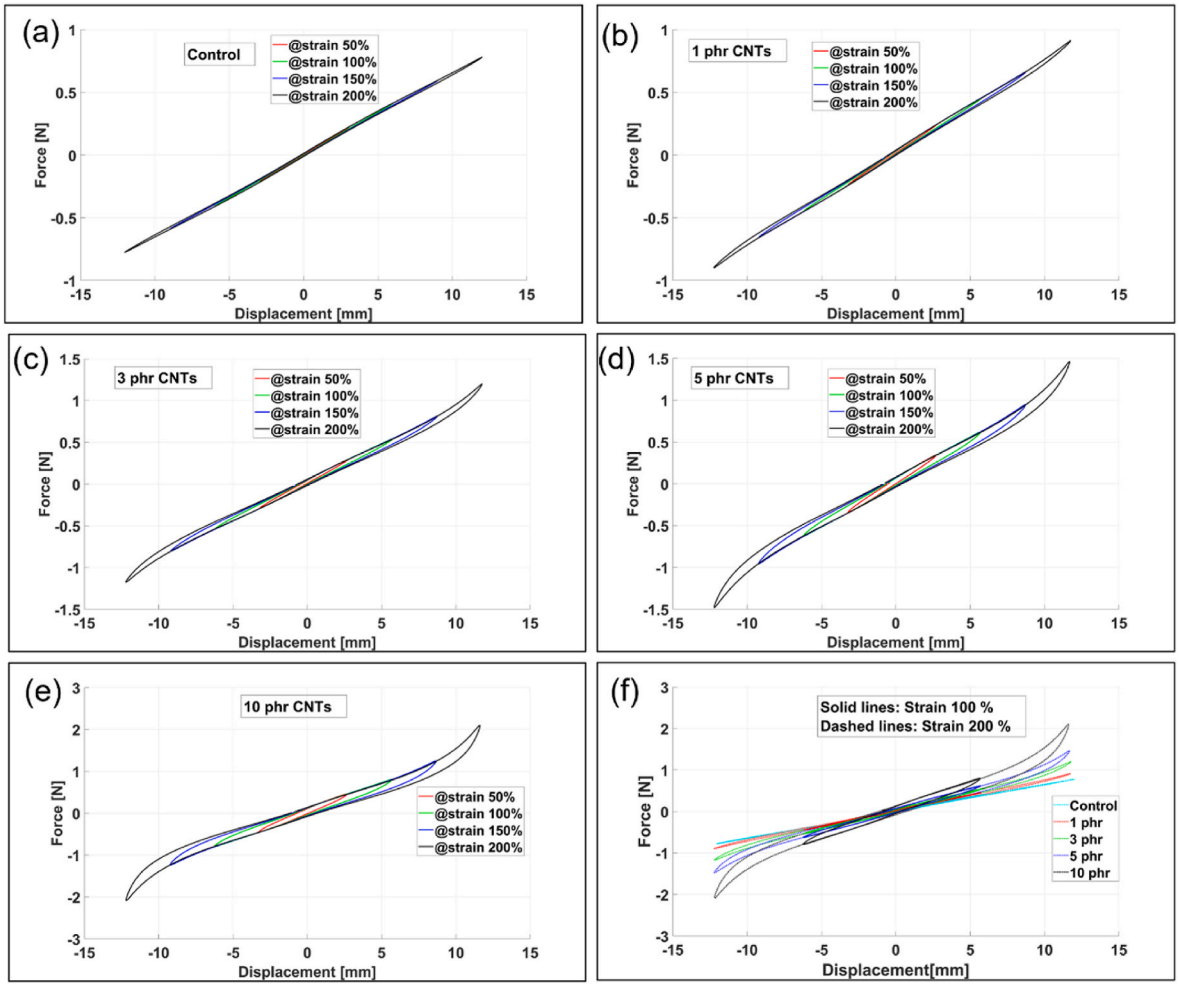

Fig. 10. Comparison of hysteresis loop as a function of strain amplitude: (a) 1Control, (b) 1 phr CNTs, (c) 3 phr CNTs, (d) 5 phr CNTs, (e) 10 phr CNTs, (f) hysteresis loop in various CNTs contents and strain amplitudes.

increasing the strain amplitude. The hysteresis loss of the neat rubber is quite negligible at small strain amplitude (<50%) demonstrating a low energy dissipation as shown in Fig. 10a and f due to an absence of CNTs. Apart from the control, increasing the strain amplitude for each nanocomposite rubber results in more nonlinearity as shown in Fig. 10 b-f. That is the hysteresis shape transforms from elliptical shape for the control and 1 phr CNTs to a relatively a nonlinear hysteresis loop for the higher CNTs loading (>3 phr). This can be ascribed to severe breakdown of the CNTs networks during large deformations [43] and strain-induced crystallization effect [44]. It can be concluded that increasing strain

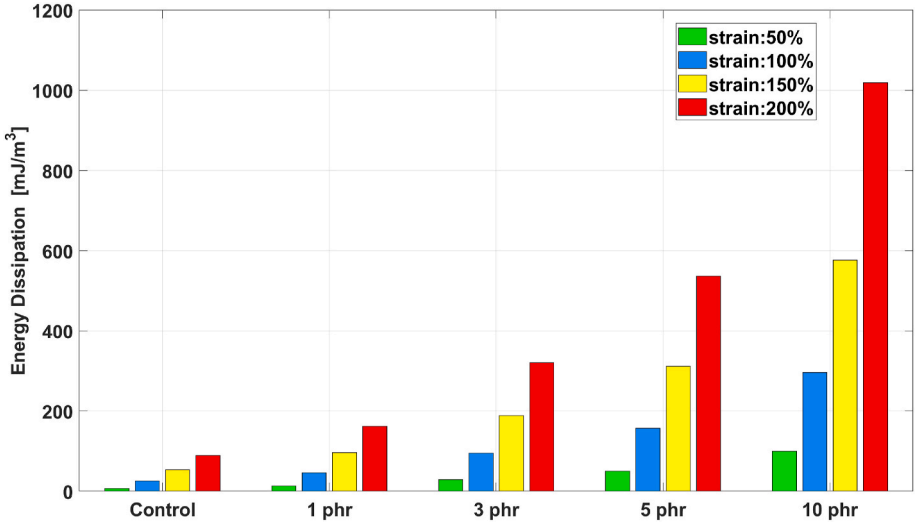

Fig. 11. Energy dissipation for different CNTs loading and various strain amplitudes.

amplitude results in a higher hysteresis loss for high CNTs loading as shown in Fig. 13 which is consistent with the literature [45].

The energy dissipation/m^3 of the rubbers, i.e., the area of the hysteresis loop presented in Fig. 9 for each strain amplitude, is shown in Fig. 11. An increase of 1040% in energy dissipation for 10 phr with respect to the control at strain amplitude of 200% is achieved. Finally, one can define what CNTs content should be used depending on the applications i.e., higher CNTs loading can be used to reach good mechanical properties as well as proper damping capabilities for soundproofing applications, However, a balanced mechanical and energy dissipation properties can be achieved using a relatively lower amount of CNTs for wave energy applications.

4. Conclusion

Rubber-based materials have a wide range of applications. Reinforcement materials could potentially reduce the total weight and volume of rubber required for the same functionality. Therefore, in this study, the inclusion of CNT was considered to establish a material baseline for a wide range of uses. CNTs-based natural nanocomposites were prepared using a combined compounding technique to guarantee a homogenous CNTs dispersion was achieved. Different CNTs content including 1 phr, 3 phr, 5 phr, and 10 phr were prepared. The Mooney viscosity, rheometry, and TEM methods were used to establish the material characterization together with a cyclic double-bonded shear test for the mechanical characterization. In summary, the following outcomes were drawn:

- A good CNT dispersion was achieved at 3 phr CNTs loading whereas increasing CNTs content resulted in the presence of both CNTs aggregates and poor CNTs-region.
- Addition of CNTs into natural rubber caused higher torque, temperature, and consequently higher energy consumption resulting from higher shear forces during mixing. The torque-time trend increased significantly at the beginning of mixing followed by a decrease and finally reached a plateau which can be attributed to further homogenization of the compound in the last stage.
- Incorporation of CNTs enhanced the viscosity up to 200% at 10 phr CNT with respect to the control batch whereas a remarkable reduction in the cured rubbers (batch1-5) compared to MB and pristine CV60 were distinguished resulting from extra processing of the former by mixer and twin-roll mill.
- The scorch time (ts2) diminished as a function of CNTs loading indicating premature vulcanization for filled rubber with respect to the control. Similarly, t90 and t95 decreased as a function of CNTs increase. The ML and MH raised in filled rubbers compared to the control manifesting enhancement of the stiffness in the filled rubber during cross-linking. The cross-link density increased with the CNTs addition.
- The incorporation of CNTs into natural rubber increased dynamic modulus, storage modulus, loss modulus, and loss angles of the materials. Sample containing 10 phr CNTs reached the highest mechanical properties in which a maximum increase of 201%, 1232%, 202%, and 339% in the storage modulus, loss modulus, complex modulus, and loss angle, respectively, are achieved in comparison with the virgin rubber.
- The presence of the Payne effect was notable at low strain amplitude in which the storage modulus remarkably dropped by strain increase (strain <10%). On the other hand, the Mullins and stress-softening effect were more tangible at intermediate strain level which led to successive reduction of the loading-unloading curve in the first two cycles and reached to stabilized state from 5th cycle onward.
- Cyclic loading was used to understand the hysteresis loop changes with CNT loading. Data was examined at an identical point in the loading history for each formulation. The loading-unloading curve was more nonlinear at higher strain amplitude for higher CNT loadings, which was attributed to more pronounced Mullins and strain-induced crystallization effects. The nonlinearity was more significant at higher CNTs content. Damping capability of the materials increased in response to CNT addition where an increase of 1040% in energy dissipation for 10 phr with respect to the control at a strain amplitude of 200% was achieved.

5. Future work

It was proved that CNTs can be beneficial in improving mechanical properties of natural rubber subjected to dynamic shear loading condition. Since NR is widely used within flexible wave energy converter devices in a harsh sea water environment [1], further investigation needs to be carried out to study the fatigue life and energy harvesting efficiency of the CNT filled rubber in muti-axial loading scenario. This is quite critical to reduce the cost for wave energy harvesting and make it more competitive with other renewable energy resources such as wind and solar energy.

Credit author statement

Ali Esmaeili: Methodology, Original Draft Preparation, Investigation, **Ian Masters**: Conceptualization, Writing, Editing, Fund acquisition, **Mokarram Hossain**: Conceptualization, Writing, Editing, Fund acquisition, Project Administration.

Declaration of competing interest

The authors declare that they have no known competing financial interests or personal relationships that could have appeared to influence the work reported in this paper.

Data availability

Data will be made available on request.

Acknowledgements

This study is funded by the Swansea Bay City Deal and the European Regional Development Fund through the Welsh European Funding Office. This study is also supported by EPSRC through the Supergen ORE Hub (EP/S000747/1), who have awarded funding for the Flexible Fund project Submerged bi-axial fatigue analysis for Flexible membrane Wave Energy Converters (FF2021-1036).

References

[1] I. Collins, M. Hossain, W. Dettmer, I. Masters, Flexible membrane structures for wave energy harvesting: a review of the developments, materials and computational modelling approaches, Renew. Sustain. Energy Rev. 151 (2021), 111478, https://doi.org/10.1016/j.rser.2021.111478.

[2] X.H. Long, Y.T. Ma, R. Yue, J. Fan, Experimental study on impact behaviors of rubber shock absorbers, Construct. Build. Mater. 173 (2018) 718–729, https://doi.org/10.1016/j.conbuildmat.2018.04.077.

[3] S. Sattayanurak, K. Sahakaro, W. Kaewsakul, W.K. Dierkes, L.A.E.M. Reuvekamp, A. Blume, J.W.M. Noordermeer, Synergistic effect by high specific surface area carbon black as secondary filler in silica reinforced natural rubber tire tread compounds, Polym. Test. 81 (2020), 106173, https://doi.org/10.1016/j.polymertesting.2019.106173.

[4] T. Yang, L. Hu, X. Xiong, M. Petrů, M.T. Noman, R. Mishra, J. Militký, Sound absorption properties of natural fibers: a review, Sustain. Times 12 (2020) 1–25, https://doi.org/10.3390/su12208477.

[5] M. Sasso, G. Palmieri, G. Chiappini, D. Amodio, Characterization of hyperelastic rubber-like materials by biaxial and uniaxial stretching tests based on optical methods, Polym. Test. 27 (2008) 995–1004, https://doi.org/10.1016/j.polymertesting.2008.09.001.

[6] F. Laraba-Abbesa, P. Ienny, R. Piques, A new “tailor-made” methodology for the mechanical behaviour analysis of rubber-like materials: II. Application to the hyperelastic behaviour characterization of a carbon-black filled natural rubber vulcanizate, Polymer (Guildf) 44 (2002) 821–840, https://doi.org/10.1016/S0032-3861(02)00719-X.

[7] S.K. Thomas, P. Dileep, P.M.S. Begum, Green polymer nanocomposites based on natural rubber and nanocellulose whiskers from Acacia caesia: mechanical, thermal, and diffusion properties, Mater, Today Proc. 51 (2022) 2444–2449, https://doi.org/10.1016/j.matpr.2021.11.613.
[8] W.P. Flauzino Neto, M. Mariano, I.S.V. da Silva, H.A. Silvério, J.L. Putaux, H. Otaguro, D. Pasquini, A. Dufresne, Mechanical properties of natural rubber nanocomposites reinforced with high aspect ratio cellulose nanocrystals isolated from soy hulls, Carbohydr. Polym. 153 (2016) 143–152, https://doi.org/10.1016/j.carbpol.2016.07.073.
[9] X. Zhang, Z. Chen, J. Li, X. Wu, J. Lin, S. He, Mechanical performance design via regulating the interactions in acrylonitrile-butadiene rubber/clay nanocomposites by small molecule compounds, Polym. Test. 110 (2022), 107565, https://doi.org/10.1016/j.polymertesting.2022.107565.
[10] F. Danafar, M. Kalantari, A review of natural rubber nanocomposites based on carbon nanotubes, J. Rubber Res. 21 (2018) 293–310, https://doi.org/10.1007/bf03449176.
[11] Z. Peng, C. Feng, Y. Luo, Y. Li, Z. Yi, L.X. Kong, Natural rubber/multiwalled carbon nanotube composites developed with a combined self-assembly and latex compounding technique, J. Appl. Polym. Sci. 125 (2012) 3920–3928, https://doi.org/10.1002/app.36389.
[12] T. Jose, G. Moni, S. Salini, A.J. Raju, J.J. George, S.C. George, Multifunctional multi-walled carbon nanotube reinforced natural rubber nanocomposites, Ind. Crop. Prod. 105 (2017) 63–73, https://doi.org/10.1016/j.indcrop.2017.04.047.
[13] A.A. Abdullateef, S.P. Thomas, M.A. Al-Harthi, S.K. De, S. Bandyopadhyay, A. A. Basfar, M.A. Atieh, Natural rubber nanocomposites with functionalized carbon nanotubes: mechanical, dynamic mechanical, and morphology studies, J. Appl. Polym. Sci. 125 (2012), https://doi.org/10.1002/app.35021.
[14] P. Selvin Thomas, A.A. Abdullateef, M.A. Al-Harthi, M.A. Atieh, S.K. De, M. Rahaman, T.K. Chaki, D. Khastgir, S. Bandyopadhyay, Electrical properties of natural rubber nanocomposites: effect of 1-octadecanol functionalization of carbon nanotubes, J. Mater. Sci. 47 (2012) 3344–3349, https://doi.org/10.1007/s10853-011-6174-4.
[15] G. Sui, W. Zhong, X. Yang, S. Zhao, Processing and material characteristics of a carbon-nanotube-reinforced natural rubber, Macromol. Mater. Eng. 292 (2007) 1020–1026, https://doi.org/10.1002/mame.200700126.
[16] H. Guo, P. Ji, I.Z. Halász, D.Z. Pirityi, T. Bárány, Z. Xu, L. Zheng, L. Zhang, L. Liu, S. Wen, Enhanced fatigue and durability properties of natural rubber composites reinforced with carbon nanotubes and graphene oxide, Materials 13 (2020) 1–12, https://doi.org/10.3390/ma13245746.
[17] B. Dong, C. Liu, Y. Lu, Y. Wu, Synergistic effects of carbon nanotubes and carbon black on the fracture and fatigue resistance of natural rubber composites, J. Appl. Polym. Sci. 132 (2015) 1–8, https://doi.org/10.1002/app.42075.
[18] H. Li, L. Yang, G. Weng, W. Xing, J. Wu, G. Huang, Toughening rubbers with a hybrid filler network of graphene and carbon nanotubes, J. Mater. Chem. A. 3 (2015) 22385–22392, https://doi.org/10.1039/c5ta05836h.
[19] B. Dong, L. Zhang, Y. Wu, Influences of different dimensional carbon-based nanofillers on fracture and fatigue resistance of natural rubber composites, Polym. Test. 63 (2017) 281–288, https://doi.org/10.1016/j.polymertesting.2017.08.035.
[20] A.S. Sethulekshmi, A. Saritha, K. Joseph, A comprehensive review on the recent advancements in natural rubber nanocomposites, Int. J. Biol. Macromol. 194 (2022) 819–842, https://doi.org/10.1016/j.ijbiomac.2021.11.134.
[21] B. Mensah, H.G. Kim, J.H. Lee, S. Arepalli, C. Nah, Carbon nanotube-reinforced elastomeric nanocomposites: a review, Int. J. Smart Nano Mater. 6 (2015) 211–238, https://doi.org/10.1080/19475411.2015.1121632.
[22] A. Fakhru'l-Razi, M.A. Atieh, N. Girun, T.G. Chuah, M. El-Sadig, D.R.A. Biak, Effect of multi-wall carbon nanotubes on the mechanical properties of natural rubber, Compos. Struct. 75 (2006) 496–500, https://doi.org/10.1016/j.compstruct.2006.04.035.
[23] L.P. Lim, J.C. Juan, N.M. Huang, L.K. Goh, F.P. Leng, Y.Y. Loh, Effect of graphene oxide particle size on the tensile strength and stability of natural rubber graphene composite, Mater. Sci. Eng. B Solid-State Mater. Adv. Technol. 262 (2020), 114762, https://doi.org/10.1016/j.mseb.2020.114762.
[24] L. Wu, P. Qu, R. Zhou, B. Wang, S. Liao, Green synthesis of reduced graphene oxide and its reinforcing effect on natural rubber composites, High Perform. Polym. 27 (2015) 486–496, https://doi.org/10.1177/0954008314555530.
[25] O. Saravari, A. Boonmahitthisud, W. Satitnaithum, S. Chuayjuljit, Mechanical and electrical properties of natural rubber/carbon nanotube nanocomposites prepared by latex compounding, Adv. Mater. Res. 664 (2013) 543–546. https://dx.doi.org/10.4028/www.scientific.net/AMR.664.543.
[26] Z. Peng, C. Feng, Y. Luo, Y. Li, L.X. Kong, Self-assembled natural rubber/multi-walled carbon nanotube composites using latex compounding techniques, Carbon N. Y. 48 (2010) 4497–4503, https://doi.org/10.1016/j.carbon.2010.08.025.
[27] L. Qu, G. Huang, P. Zhang, Y. Nie, G. Weng, J. Wu, Synergistic reinforcement of nanoclay and carbon black in natural rubber, Polym. Int. 59 (2010) 1397–1402, https://doi.org/10.1002/pi.2881.
[28] S. Agnelli, S. Pandini, A. Serafini, S. Musto, M. Galimberti, Anisotropic nonlinear mechanical behavior in carbon nanotubes/poly(1,4-cis-isoprene) nanocomposites, Macromolecules 49 (2016) 8686–8696, https://doi.org/10.1021/acs.macromol.6b01682.
[29] G. Prioglio, S. Agnelli, S. Pandini, M. Galimberti, Silica-based composites with enhanced rheological properties thanks to a nanosized graphite functionalized with serinol pyrrole, Appl. Sci. 11 (2021), https://doi.org/10.3390/app112311410.
[30] R. Ismail, A. Ibrahim, M. Rusop, A. Adnan, Determination of mechanical properties natural rubber compounds using double shear test pieces, Int. J. Civ. Eng. Technol. 9 (2018) 37–43.
[31] H. Chougule, U. Giese, Application of Carbon NanoTubes in Specialty Rubbers –Potential and Properties, 2016, pp. 1–8. www.kgk-rubberpoint.de.
[32] N. Phuhiangpa, W. Ponloa, S. Phongphanphanee, W. Smitthipong, Performance of nano-and microcalcium carbonate in uncrosslinked natural rubber composites: new results of structure–properties relationship, Polymers 12 (2020) 1–15, https://doi.org/10.3390/polym12092002.
[33] A. Krainoi, C. Kummerlöwe, N. Vennemann, Y. Nakaramontri, S. Pichaiyut, C. Nakason, Effect of carbon nanotubes decorated with silver nanoparticles as hybrid filler on properties of natural rubber nanocomposites, J. Appl. Polym. Sci. 136 (2019), https://doi.org/10.1002/app.47281.
[34] N.M. Setyadewi, I.N. Indrajati, N. Darmawan, Mechanical properties and curing characteristics of shape memory natural rubber, in: IOP Conf. Ser. Mater. Sci. Eng., Institute of Physics Publishing, 2019, https://doi.org/10.1088/1757-899X/541/1/012012.
[35] M. Shamonin, E.Y. Kramarenko, Highly responsive magnetoactive elastomers, Nov. Magn. Nanostructures Unique Prop. Appl. (2018) 221–245, https://doi.org/10.1016/B978-0-12-813594-5.00007-2.
[36] S.K. Srivastava, Y.K. Mishra, Nanocarbon reinforced rubber nanocomposites: detailed insights about mechanical, dynamical mechanical properties, payne, and mullin effects, Nanomaterials 8 (2018) 1–56, https://doi.org/10.3390/nano8110945.
[37] C. Xue, H. Gao, G. Hu, Viscoelastic and fatigue properties of graphene and carbon black hybrid structure filled natural rubber composites under alternating loading, Construct. Build. Mater. 265 (2020), 120299, https://doi.org/10.1016/j.conbuildmat.2020.120299.
[38] K. Song, Interphase Characterization in Rubber Nanocomposites, Elsevier Ltd, 2017, https://doi.org/10.1016/B978-0-08-100409-8.00004-8.
[39] R. Kaltseis, C. Keplinger, S.J. Adrian Koh, R. Baumgartner, Y.F. Goh, W.H. Ng, A. Kogler, A. Tröls, C.C. Foo, Z. Suo, S. Bauer, Natural rubber for sustainable high-power electrical energy generation, RSC Adv. 4 (2014) 27905–27913, https://doi.org/10.1039/c4ra03090g.
[40] Z. Yang, H. Peng, W. Wang, T. Liu, Crystallization behavior of poly (ε-caprolactone)/layered double hydroxide nanocomposites, J. Appl. Polym. Sci. 116 (2010) 2658–2667, https://doi.org/10.1002/app.
[41] T.T. Mai, Y. Morishita, K. Urayama, Novel features of the Mullins effect in filled elastomers revealed by stretching measurements in various geometries, Soft Matter 13 (2017) 1966–1977, https://doi.org/10.1039/c6sm02833k.
[42] S. Cantournet, R. Desmorat, J. Besson, Mullins effect and cyclic stress softening of filled elastomers by internal sliding and friction thermodynamics model, Int. J. Solid Struct. 46 (2009) 2255–2264, https://doi.org/10.1016/j.ijsolstr.2008.12.025.
[43] L. Wei, X. Fu, M. Luo, Z. Xie, C. Huang, J. Zhou, Y. Zhu, G. Huang, J. Wu, Synergistic effect of CB and GO/CNT hybrid fillers on the mechanical properties and fatigue behavior of NR composites, RSC Adv. 8 (2018) 10573–10581, https://doi.org/10.1039/c7ra12830d.
[44] A. Masa, S. Iimori, R. Saito, H. Saito, T. Sakai, A. Kaesaman, N. Lopattananon, Strain-induced crystallization behavior of phenolic resin crosslinked natural rubber/clay nanocomposites, J. Appl. Polym. Sci. 132 (2015), https://doi.org/10.1002/app.42580.
[45] H. Kahraman, E. Haberstroh, Mechanical characterisation of anisotropic stress softening in carbon black filled rubber, Plast., Rubber Compos. 42 (2013) 19–25, https://doi.org/10.1179/1743289812Y.0000000026.